ACCOUNTS of chemical research

Article

pubs.acs.org/accounts

The Importance of Ensemble Averaging in Enzyme Kinetics

Published as part of the Accounts of Chemical Research special issue "Protein Motion in Catalysis".

Laura Masgrau[†] and Donald G. Truhlar*[,‡]

[†]Institut de Biotecnologia i de Biomedicina, Universitat Autònoma de Barcelona, 08193 Bellaterra (Barcelona), Spain

[‡]Department of Chemistry, Chemical Theory Center, and Supercomputing Institute, University of Minnesota, 207 Pleasant St. SE, Minneapolis, Minnesota 55455-0431, United States

CONSPECTUS: The active site of an enzyme is surrounded by a fluctuating environment of protein and solvent conformational states, and a realistic calculation of chemical reaction rates and kinetic isotope effects of enzyme-catalyzed reactions must take account of this environmental diversity. Ensemble-averaged variational transition state theory with multidimensional tunneling (EA-VTST/MT) was developed as a way to carry out such calculations. This theory incorporates ensemble averaging, quantized vibrational energies, energy, tunneling, and recrossing of transition state dividing surfaces in a systematic way. It has been applied successfully to a number of hydrogen-, proton-, and hydride-transfer reactions. The theory also exposes the set of effects that should be considered in reliable rate constants calculations.

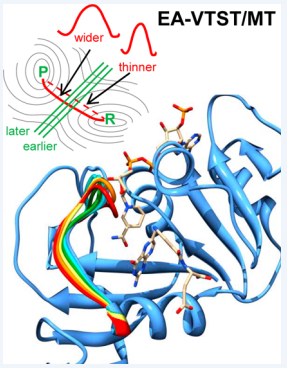

We first review the basic theory and the steps in the calculation. A key role is played by the generalized free energy of activation profile, which is obtained by quantizing the classical potential of mean force as a function of a reaction coordinate because the one-way flux through the transition state dividing surface can be written in terms of the generalized free energy of activation. A recrossing transmission coefficient accounts for the difference between the one-way flux through the chosen transition state dividing surface and the net flux, and a tunneling transmission coefficient converts classical motion along the reaction coordinate to quantum mechanical motion. The tunneling calculation is multidimensional, accounting for the change in vibrational frequencies along the tunneling path and shortening of the tunneling path with respect to the minimum energy path (MEP), as promoted by reaction-path curvature. The generalized free energy of activation and the transmission coefficients both involve averaging over an ensemble of reaction paths and conformations, and this includes the coupling of protein motions to the rearrangement of chemical bonds in a statistical mechanically correct way. The standard deviations of the transmissions coefficients provide information on the diversity of the distribution of reaction paths, barriers, and protein conformations along the members of an ensemble of reaction paths passing through the transition state.

We first illustrate the theory by discussing the application to both wild-type and mutant *Escherichia coli* dihydrofolate reductase and hyperthermophilic *Thermotoga maritima* dihydrofolate reductase (DHFR); DHFR is of special interest because the protein conformational changes have been widely studied. Then we present shorter discussions of several other applications of EA-VTST/MT to transfer of protons, hydrogen atoms, and hydride ions and their deuterated analogs. Systems discussed include hydride transfer in alcohol dehydrogenase, xylose isomerase, and thymidylate synthase, proton transfer in methylamine dehydrogenase, hydrogen atom transfer in methylmalonyl-CoA mutase, and nucleophilic substitution in haloalkane dehalogenase and two-dimensional potentials of mean force for potentially coupled proton and hydride transfer in the β-oxidation of butyryl-coenzyme A catalyzed by short-chain acyl-CoA dehydrogenase and in the pyruvate to lactate transformation catalyzed by lactate dehydrogenase.

1. INTRODUCTION

Conformational changes of enzymes and their substrates during the catalytic cycle have now been identified for many systems.[1,2] Such changes raise the question of how protein motions affect the chemical step.[3−8] Some authors emphasize protein-promoting motions dynamically modulating the shape of the potential energy barrier and driving a reaction dominated by tunneling.[8−11] Others, while not neglecting tunneling, emphasize that enzyme catalysis is achieved primarily by reducing the activation free energy, which is dominated by quasiequilibrium components that represent the flux through a transition state dividing surface but also have contributions from recrossing dynamics and tunneling.[3,12]

Many models for enzyme kinetics have been developed.[8,13−17] Here we review ensemble-averaged variational transition state theory with multidimensional tunneling (EA-VTST/MT).[13,18,19] This theory incorporates zero point energy, tunneling, and recrossing in a systematic way. Because it accounts for quantum mechanical effects, the theory can be used to calculate accurate rate constants for hydrogen-, proton-, and hydride-transfer reactions and the associated kinetic isotope effects (KIEs)[20] (the latter being experimental tools for elucidating reaction mechanisms and gaining information

Received: August 28, 2014
Published: December 24, 2014

DOI: 10.1021/ar500319e
Acc. Chem. Res. 2015, 48, 431−438

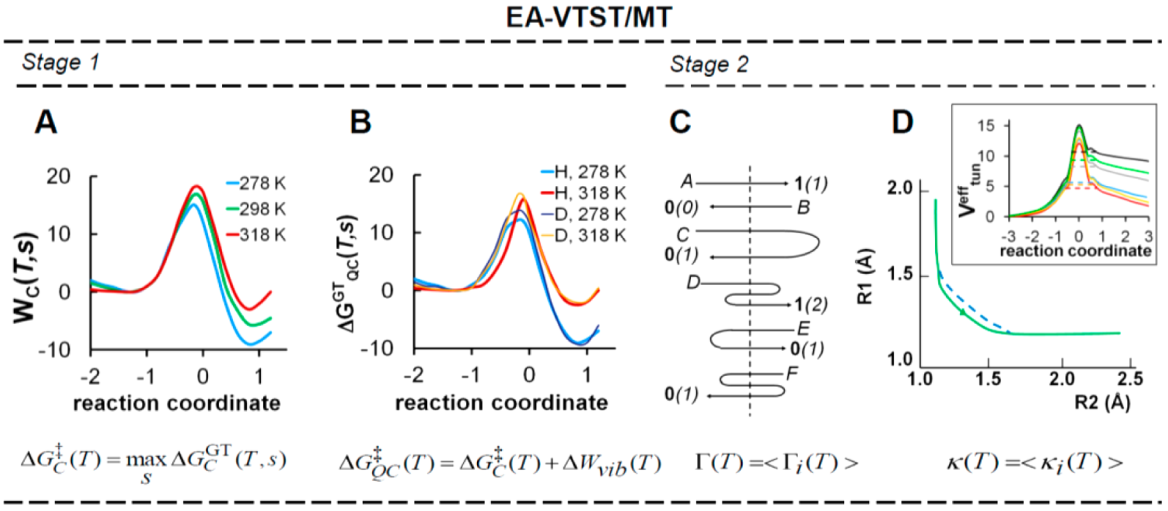

Figure 1. Schematic representation of the steps of an EA-VTST/MT calculation. (A) Classical potentials of mean force ($W_C(T)$) along a selected reaction coordinate. (B) Inclusion of quantal vibrational free energies, which introduces differences between isotopes that can vary with temperature. (C) Trajectories underlying the recrossing transmission coefficient with counts of reactive events first, then forward crossings of the TS in parentheses. (D) A tunneling path (dotted line) and the longer MEP (solid line) underlying the tunneling transmission coefficient. The inset shows barriers for various conformations and the representative tunneling energy for each of them, from ref 74. Energies are in kcal/mol.

about transition states). We will discuss modeling the chemical step in enzyme catalysis, but the theory could also be used for other steps, such as product release, or in fact for any reaction in condensed-phase media. We believe this is an appropriate time for this Account because the questions of ensemble averaging and conformational dynamics are receiving increasing attention in the context of enzyme kinetics.[21]

Computational enzyme kinetics requires a potential energy function (or its gradient, equivalent to a force field) and dynamical methods for treating the various elementary steps of the mechanism. This Account is about the reactive dynamics of the chemical step. Suitable force fields for reactive dynamics are calculated by treating the active site molecules or fragments by a selected quantum mechanical electronic structure method and the rest of the system by molecular mechanics, as reviewed elsewhere[22−24] (such treatments are called combined QM/MM methods). The choice of QM method often made in work carried out so far is semiempirical molecular orbital theory with specific reaction parameters.[25]

2. EA-VTST/MT FOR THE CHEMICAL STEP IN ENZYME CATALYSIS

The phenomenological free energy of activation ($\Delta G_{act,phen}$) associated with the chemical step is derived from the experimental rate constant (k^{exp}) by

$$k^{exp}(T) = \frac{k_B T}{h} \exp\left[\frac{\Delta G_{act,phen}(T)}{RT}\right] \quad (1)$$

where k_B, h, R, and T are, respectively, Boltzmann's and Planck's constants, the gas constant, and temperature.

The EA-VTST/MT method and examples of its application have been presented in earlier reviews.[14,18−20,22,26,27] Here we will explain the steps in a calculation of k^{exp} or $\Delta G_{act,phen}$ and relate them to protein motion. EA-VTST/MT is based on transition state theory (TST),[28] in particular, on canonical variational transition state theory (CVT).[29] TST first assumes that a Born−Oppenheimer potential energy surface governs the system under study. Then it makes the fundamental assumptions that trajectories originate from an equilibrated reactant and that no trajectories recross a hypersurface in phase space that divides the reactant region from the product region. This hypersurface is called the transition state (TS), and in condensed-phase systems, it has coordinate-space dimensionality of $3N - 1$, where N is the number of atoms of the system treated explicitly (additional atoms, which may include most of the protein and solvent, are treated as an equilibrated environment); atoms treated explicitly are called the primary subsystem. Notice that the TS has one degree of freedom less that the reactants; this is the reaction coordinate. The no recrossing assumption would be valid if the reaction coordinate were indeed separable from the other degrees of freedom. A simple way to calculate the one-way flux through the TS is to convert it to a calculation of a quasithermodynamic free energy of activation.[30] This yields

$$k^{QC}(T) = \frac{k_B T}{h} \exp\left[\frac{\Delta G_{QC}^{\ddagger}(T)}{RT}\right] \quad (2)$$

where $\Delta G_{QC}^{\ddagger}$ is the free energy difference between the $(3N - 1)$-dimensional TS and the $3N$-dimensional reactants. Although the derivation of eq 2 is classical, we calculate $\Delta G_{QC}^{\ddagger}$ with quantized vibrational levels,[31] so we call this free energy difference and rate constant quasiclassical (QC).

If transitions among sets of reactant states are slow compared with chemical reaction, then the slowly interconverting sets of reactant states should be treated as separate reactants in a multispecies mechanism.[32] Here, however, we consider the case where conformational transitions among reactant states occur on a faster time scale than chemical reaction; under such conditions the assumption of a single well-equilibrated reactant is reasonable;[3] however the assumption that there is no recrossing can be violated. Furthermore, at this point the reaction coordinate is still classical (because it is missing in $\Delta G_{QC}^{\ddagger}$, which we quantized). Recrossing and quantal reaction-coordinate motion (which includes both tunneling and wave-like nonclassical reflection at energies above the barrier) can be included by a multiplicative transmission coefficient:

DOI: 10.1021/ar500319e
Acc. Chem. Res. 2015, 48, 431−438

$$k^{\ddagger}(T) = \gamma(T)k^{QC}(T) \quad (3)$$

with $\gamma(T)$ being the transmission coefficient given by

$$\gamma(T) = \Gamma(T)\kappa(T) \quad (4)$$

where Γ accounts for recrossing and κ accounts for nonclassical reaction-coordinate motion. Since the effect of tunneling is usually much larger than the effect of nonclassical reflection, we usually just refer to κ as the tunneling transmission coefficient. In general, $\Gamma \leq 1$, and κ is usually greater than 1.

By comparison of eqs 1 and 3, the computed phenomenological free energy of activation ($\Delta G^{\ddagger}_{act,phen}$) is calculated as

$$\Delta G^{\ddagger}_{act,phen}(T) = -RT\ln(\gamma(T)) + \Delta G^{\ddagger}_{QC}(T) = \Delta G^{\ddagger}_{\gamma}(T) + \Delta G^{\ddagger}_{QC}(T) \quad (5)$$

where

$$\Delta G^{\ddagger}_{\gamma}(T) = -RT\ln(\Gamma(T)) - RT\ln(\kappa(T)) = \Delta G^{\ddagger}_{recross}(T) + \Delta G^{\ddagger}_{tun}(T) \quad (6)$$

Next we summarize the steps[13] in calculating $\Delta G^{\ddagger}_{QC}$, Γ, and κ. In stage 1, we calculate $\Delta G^{\ddagger}_{QC}$, and in stage 2, we compute γ (Figure 1).

Stage 1 starts with the calculation of the one-dimensional classical potential of mean force, W_C, along a chosen reaction coordinate s. This is usually done by umbrella sampling calculations[33,34] with a reaction coordinate involving the bond distances that define the chemical transformation (but other reaction coordinate definitions can also be used[35]). The potential of mean force as a function of s yields the generalized transition-state (GT) free energy of activation profile via

$$\Delta G^{GT}_{C}(T, s) = W_C(T, s) - [W_C(T, s = s^R) + G^R_{C,F}(T)] \quad (7)$$

where C denotes classical, R denotes the reactant, and the last term is the contribution of the reaction coordinate F at the reactant. Equation 7 includes thermal and entropic contributions due to equilibrium fluctuations, including protein conformational changes as the system responds to the reaction progress variable s. The maximum of eq 7 as a function of s can define the classical TS. Notice that the location of the classical TS may vary with temperature (Figure 1A).[20,36,37]

Although the calculations so far have usually been performed on a QM/MM potential energy surface,[22−24] the motion of the atoms is treated up to this point by classical dynamics, which is why we attach the label C. In step 2 of stage 1, quantization effects on the vibrational free energy are included to convert eq 7 to a quasiclassical generalized free energy of activation by adding a term that converts the vibrational free energy of the primary system from classical to quantal (Figure 1B):

$$\Delta G^{GT}_{QC}(T, s) = \Delta G^{GT}_{C}(T, s) + \Delta W_{vib}(T, s) \quad (8)$$

The correction term is calculated by performing (for multiple configurations of the system at each sampled value of s) instantaneous normal-mode analysis of the primary-subsystem modes orthogonal to the reaction coordinate.[13,31] The maximum of $\Delta G^{GT}_{QC}(T,s)$ is chosen as the transition state; thus

$$\Delta G^{\ddagger}_{QC}(T) = \max_{s} \Delta G^{GT}_{QC}(T, s) \quad (9)$$

In stage 2, we calculate Γ and κ (Figures 1C,D). Configurations are sampled from the quasiclassical TS ensemble, and the isoinertial minimum energy path (MEP) for each of them is calculated for the primary atoms keeping the rest of the system (secondary zone) frozen; this is called the static-secondary-zone approximation (SSZ).[13,19] Recrossing and tunneling transmission coefficients are calculated for the reaction swath associated with each of these MEPs. Explicit couplings of the environment degrees of freedom to the reaction coordinate are thereby introduced at this stage, as conformation-specific reaction coordinates and tunneling paths are calculated for each selected enzyme configuration and are used to compute ensemble averaged Γ and κ coefficients. Relaxation of the secondary-zone atoms in the calculation of the transmission coefficients could also be included in a third stage (equilibrium-secondary-zone approximation, ESZ).[13,19]

In principle the ensemble averaged over is the canonical one, but that ideal limit is reached only for infinitely long sampling times. Special techniques could be introduced for sampling over slowly interconverting regions[38] of reactant space.

Note that the recrossing transmission coefficient has sometimes been calculated by trajectory calculations. Trajectories are less accurate than VTST because they do not enforce zero point constraints. These constraints would be exact if modes transverse to the reaction coordinate were vibrationally adiabatic, and they are known to be important[39] at dynamical bottlenecks.

Computational details for calculating tunneling transmission coefficients are given elsewhere,[13,40,41] but it is important to recognize that only multidimensional tunneling (MT) approaches (e.g., ZCT, SCT, LCT, and μOMT),[29,42] are able to calculate reliable rates because the reaction coordinate is not separable even along a given path due to reaction-path curvature and the s-dependence of vibrational frequencies and generalized normal-mode directions. The optimum MT paths, which result from a compromise between short path length and low effective potential along the path, are isotope dependent and shorter than the MEP; the latter feature is called corner-cutting tunneling (Figure 1D). This coupling of the tunneling path to other coordinates has often been called vibrationally enhanced or vibrationally promoted tunneling or gated tunneling;[9] it emerges naturally in MT methods without any special assumptions.

The magnitude and standard deviation of Γ serve as indicators of the amount of coupling present and the size of the fluctuations.[14] The standard deviations of Γ and κ are not statistical errors bars but real physical characterizations of the magnitude of conformational fluctuations coupled to the reaction coordinate.

The software package CHARMMRATE,[43] which is a module of the CHARMM program,[44] has been developed to carry out the EA-VTST/MT calculations following the above scheme. This package is an interface of the CHARMM program for macromolecular simulations and the POLYATE program[45] for variational transition state theory calculations including multidimensional tunneling.

3. EXAMPLES OF APPLICATIONS

EA-VTST/MT has been used to study the atomic details of the kinetics of numerous enzymes.[13,36−38,46−58] Among them, dihydrofolate reductase (DHFR) is a paradigm system for the study of the role of protein motions in enzyme catalysis, both experimentally and theoretically, because of the well-characterized conformational changes and the measured T dependence of the KIEs.[2,5,14,59−61] EA-VTST/MT has been applied to

DOI: 10.1021/ar500319e
Acc. Chem. Res. 2015, 48, 431−438

both wild-type and mutant DHFR from different organisms.[36,37,48,56,57] Sections 3.1−3.3 review those applications. Some applications to other systems for which conformational aspects are highlighted are discussed in section 3.4.

3.1. Wild-type *Escherichia coli* Dihydrofolate Reductase (EcDHFR)

EcDHFR is a monomer that catalyzes the hydride transfer from C4 of the NADPH cofactor to N5 of 7,8-dihydrofolate (DHF) to form 5,6,7,8-tetrahydrofolate (THF).[62] Structural and NMR relaxation studies[63] showed that the M20, F−G, and G−H loops of DHFR (Figure 2) are flexible and that millisecond

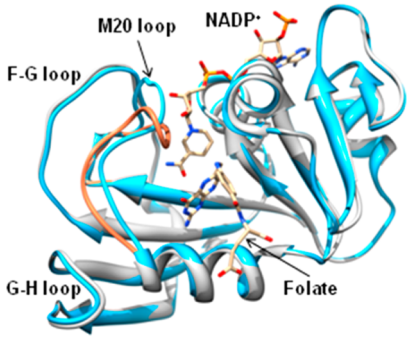

Figure 2. Superimposition of wild-type EcDHFR in the occluded (orange, PDB code 1RX4) and closed (blue, PDB code 1RX2) conformations. The M20, F−G, and G−H loops are indicated in the closed conformation containing the protonated DHF substrate and NADPH cofactor.

conformational motions accompany substrate binding and product release by switching the enzyme between the "closed" and "occluded" conformations.[64] At pH 7.0, product release is partially rate-limiting,[65] whereas at elevated pH, the hydride transfer becomes rate limiting. Rate constants and intrinsic KIEs have been obtained at physiological pH.[56,65]

EA-VTST/MT based on a QM/MM potential was applied to study the hydride-transfer step at 300 K.[48] Quantizing the vibrational free energy lowered (eq 8) the activation free energy by 2.5 kcal/mol, similarly to what has been found in other hydrogen ($H/H^-/H^+$) transfers. Thirteen enzyme configurations from the TS ensemble were used to calculate ensemble-averaged transmission coefficients and their standard deviations ($\Gamma = 0.75 \pm 0.26$, $\kappa = 3.13 \pm 1.29$, $\gamma = 2.54 \pm 1.61$). The large standard deviations of these transmission coefficients reflect significant fluctuations in the barrier heights, barrier widths, and barrier shapes among the different conformations of the enzyme. The final $\Delta G^{\ddagger}_{act,phen}$ is 13.1 kcal/mol, in very good agreement with the experimental 13.4 kcal/mol.

Good agreement with experiment was also obtained for the primary H/D KIE (theory, 2.8; experiment, 3.0), which is mainly a consequence of the quantization of bound vibrations. A 13% effect was predicted for the secondary H/D KIE, and this was confirmed by experiment[66] after the prediction. The quasiclassical value of this KIE is only 1.03, so tunneling increases the deviation from unity by more than a factor of 4.

These EA-VTST/MT calculations were based on a geometrical reaction coordinate defined in terms of substrate bond distances. With this coordinate, one was able to conveniently sample the protein conformational changes that accompany this hydride transfer, and their effect is included in $\Delta G^{\ddagger}_{act,phen}$.[48] Agarwal et al. had studied the same reaction by other approaches with an energy gap reaction coordinate, and the recrossing transmission coefficients from the two treatments are similar, showing the suitability of both reaction coordinates.[67]

As seen in several other enzymes in their optimal temperature range, the measured primary H/D KIE[66] exhibits only a weak dependence on T. This has often been interpreted in terms of Marcus-like models of charge transfer, sometimes referred to as environmentally coupled tunneling or vibrationally enhanced tunneling,[9,68] and it can be explained without special assumptions by EA-VTST;[36] in particular, the magnitude of the H/D KIE for the hydride transfer catalyzed by EcDHFR and its weak temperature dependence (278−318 K) were reproduced within experimental error.[36] Two key features were identified that explain this experimental observation. Without accounting for these two factors, the KIE would have decreased 12% instead of the 6.5% calculated. The first factor is the shift along the reaction coordinate of the classical and quasiclassical TSs toward a more product-like location as the temperature increases (as exemplified in Figures 1A and 1B). This results in a greater isotopic difference in the quantized vibrational free energy of the new TS ensemble of configurations at 318 K; at this stage, the calculated KIE decreases by 1% instead of the 8% that it would have decreased with a "static" TS. Second, the barrier at 318 K is more symmetric and thinner than that at 278 K, which leads to an unusual temperature dependence of κ. The averaged transmission coefficients in Table 1 show that κ decreases with

Table 1. Averaged Transmission Coefficients Calculated for the Hydride Transfer Reaction Catalyzed by EcDHFR[a]

	278 K		318 K	
	H	D	H	D
recrossing (Γ)	0.79(0.27)	0.78(0.25)	0.85(0.21)	0.86(0.17)
tunneling (κ, μOMT)	3.77(1.94)	3.48(1.24)	2.84(0.73)	2.69(0.58)
overall (γ)	3.12(1.89)	2.74(1.16)	2.48(0.95)	2.32(0.62)

[a]From ref 36; standard deviations in parentheses.

temperature, as expected because thermally activated reactive processes become more accessible. However, a computational experiment concluded that the decrease is less pronounced (only 3%) than it would have been with an unchanged barrier shape (5%) because the mean effective tunneling potential at higher temperature has also become more symmetric and thinner.[36]

Table 1 shows that the 20 reaction paths of the TS ensemble used in the calculations at each temperature show a broad distribution of tunneling transmission coefficients. The large relative standard deviations illustrate the sensitivity of the tunneling dynamics to the environment, and the smaller relative standard deviations values at higher temperature indicate, surprisingly, smaller fluctuations at higher temperatures.

Several residues in the above-mentioned M20 loop were seen to move closer to the cofactor in going from the reactants to the TS, providing stabilization to the TS (stabilization by residues in other loops also occurs).[48,67] These changes, mainly in hydrogen bond distances, reflect changing ensemble averages of conformational substates as the system progresses along the hydride transfer coordinate from reactants to the TS, and this is included in the $\Delta G^{\ddagger}_{act,phen}$.

Recently, for wild-type and heavy (^{15}N, ^{13}C, ^{2}H substituted) EcDHFR, Luk et al.[56] used a combination of experiments and computational methods (including EA-VTST/MT with

DOI: 10.1021/ar500319e
Acc. Chem. Res. 2015, 48, 431−438

Table 2. Averaged Transmission Coefficients Calculated for TmDHFR-Catalyzed Reaction at 278, 298, and 338 K[a]

	278 K		298 K		338 K	
	H	D	H	D	H	D
recrossing (Γ)	0.66(0.29)	0.63(0.28)	0.66(0.28)	0.64(0.28)	0.79(0.21)	0.71(0.26)
tunneling (κ)	5.25(1.38)	4.92(0.89)	4.13(0.99)	3.81(0.54)	2.00(0.38)	1.97(0.52)
overall (γ)	3.38(1.74)	3.09(1.55)	2.72(1.31)	2.44(1.12)	1.64(0.66)	1.51(0.86)

[a]Data from ref 37. Averaged over 14 configurations. Standard deviations in parentheses.

recrossing transmission coefficients calculated by reactive trajectory simulations) to study the role of protein dynamics in EcDHFR catalysis. They concluded that light and heavy enzymes present the same $\Delta G^{\ddagger}_{QC}$ and tunneling contributions, with no significant participation of promoting motions in modulating the barrier or driving tunneling, and that the slightly slower rate obtained for the heavy enzyme arises from recrossing.

3.2. Mutant Enzymes of EcDHFR

Enzyme KIEs and the framework of EA-VTST/MT have been used to study the N23PP/S148A mutant of EcDHFR,[57] which does not present the millisecond-to-microsecond time scale motions observed in the M20 loop of wild-type EcDHFR and which displays a reduced hydride transfer rate constant. The main reason is an increase in $\Delta G^{\ddagger}_{QC}$ due to a greater reorganization energy required to set up active site for hydride transfer catalysis in the mutant; a slightly higher degree of recrossing was also obtained.[57] Interestingly, the mutant enzyme exhibited higher flexibility on the femtosecond time scale. Fan et al. computed the H/D KIE for M24W/G121V EcDHFR at three different temperatures and concluded that reduced dynamic flexibility of the M20 loop at the TS resulted in a reduced entropy of activation leading to a higher free energy barrier, resulting in the slower rate measured in the mutant.[69]

3.3. *Thermotoga maritima* DHFR (TmDHFR)

The hydride transfer rate constant and the T dependence of the H/D primary KIEs have also been measured for hyperthermophilic TmDHFR. The chemical step is slower than that for EcDHFR, and the KIEs show a biphasic temperature dependence (highly T-dependent below 289 K but nearly T-independent at high temperatures).[70] TmDHFR exists as a homodimer in which interface hydrogen-bond interactions lock the FG loop in a conformation that prevents it from adopting the "closed" conformation observed in EcDHFR. EA-VTST/MT studies were performed for this enzyme[37] and yielded significant changes with temperature of the free energy barrier shape, the TS location, and the standard deviations of the transmission coefficients (Table 2), as for the EcDHFR system.[36] It was also found that dimerization contributes to enzyme catalysis. $\Delta G^{\ddagger}_{C}(T)$ and $\Delta G^{\ddagger}_{QC}(T)$ were found to be higher for TmDHFR than for EcDHFR but with Γ and κ slightly higher and showing slightly smaller fluctuations. Very recently, a light-enzyme/heavy-enzyme KIE of essentially unity has been reported for TmDHFR,[71] and this was interpreted as an indication that this enzyme, unusually but probably because of the same factors that promote its thermal stability, has negligible coupling of protein motions and conformational changes to the steps in the catalytic mechanism.

3.4. Other Examples

Hydride transfer catalyzed by alcohol dehydrogenase was the first enzyme studied within the full framework of EA-VTST/MT.[13] One-dimensional tunneling models had been unable to simultaneously reproduce the primary and secondary KIEs, but the use of multidimensional tunneling succeeded, providing dramatic confirmation of the importance of isotope-dependent corner cutting for determining accurate κ and KIE values.

H/D KIEs of ~18 have been measured for the proton transfer catalyzed by methylamine dehydrogenase (MADH).[9,72] This value was well-reproduced by EA-VTST/MT calculations. Multidimensional tunneling provides large rate enhancement (κ_H = 84).[46] Detailed analysis of the tunneling paths and effective potentials for different configurations of the system provided insight into the tunneling process.[46,73,74] The inset in Figure 1D shows six MEPs used in the calculation of κ_H and the corresponding SCT representative tunneling energies, which are the energies at which tunneling is most probable.[74] Notice that the foothills of the barrier are surmounted classically, followed by tunneling through the top of the barrier. Although the MADH system is similar to aromatic amine dehydrogenase (experimental KIE = 55 ± 6)[75] for partial atomic charges along the reaction path, there are important differences in the proton transfer energetics.[74−76]

Very large KIEs (50 at 278 K) have also been measured for the reaction catalyzed by methylmalonyl-CoA mutase. EA-VTST/MT calculations yielded very good agreement with experiment.[51] Standard deviations of κ were found to be small compared with the effect of reaction-path curvature, and this was interpreted as an indicator that the fluctuating coordinates coupled to the tunneling path were not from the protein environment in the secondary zone but rather from the 45-atom primary subsystem.

EA-VTST/MT was applied to study the β-oxidation of butyryl-coenzyme A catalyzed by short-chain acyl-CoA dehydrogenase.[50] Two-dimensional free energy surfaces showed that hydride transfer is the slow step. With the static-secondary-zone approximation, quite small averaged recrossing transmission coefficients were obtained (0.36 ± 0.3 for H and 0.40 ± 0.3 for D), suggesting that the environment had to be better relaxed in the stage-2 reaction coordinate. The use of the equilibrium-secondary-zone approach increased Γ_H and Γ_D to 0.86 ± 0.04 and 0.82 ± 0.01, respectively. The experimental KIE is between the values obtained by the two approaches.

The intrinsic primary KIE of the reaction catalyzed by haloalkane dehalogenase was also investigated by EA-VTST/MT calculations.[58] The recrossing transmission coefficient for the enzyme-catalyzed reaction was lower than that of the uncatalyzed reaction in solution indicating that, although it is not the dominant factor, decreased dynamical recrossing can contribute to enzyme catalysis.

The study of xylose isomerase[47,49] showed that the enzyme adopts a different conformation in the reactants and the TS of the catalyzed hydride transfer and that this makes an important contribution to $\Delta G^{\ddagger}_{QC}$. The motion of one of the two Mg^{2+} is strongly coupled to the reaction coordinate. In a related study,[77] molecular dynamics simulations provided a warning

DOI: 10.1021/ar500319e
Acc. Chem. Res. 2015, 48, 431−438

that significant differences can be observed in the ligand sphere of the Mg^{2+} when starting from apparently similar X-ray structures.

In the study of lactate dehydrogenase, Ferrer et al.[38] used a two-dimensional potential of mean force and an adaptation of EA-VTST/MT to calculate the rate constants associated with several reactant valleys differing in the conformation of an active-site loop. These different reactant complexes led to conformationally different reaction paths with different rate constants because interconversion between the different substates valleys was too slow compared with the sampling performed in the calculations. The authors discussed this in light of the dynamic disorder observed in single-molecule experiments.[78]

EA-VTST/MT calculations of the weakly *T*-dependent primary KIEs for the hydride transfer catalyzed by thymidylate synthase are in reasonable agreement with experiment.[55] Recrossing transmission coefficients were far from unity; in principle, they could be increased by a better choice of reaction coordinate, and they indicate a significant coupling between protein motions and the chosen geometric reaction coordinate.

4. CONCLUDING REMARKS

The roles of static disorder and structural fluctuations, protein dynamics, conformational selection, and multiple or diverse reactive pathways in enzyme kinetics are topics where our current understanding is advancing rapidly. Ensemble-averaged variational transition state theory with multidimensional tunneling (EA-VTST/MT) provides a general theoretical framework and a practical protocol for incorporating thermally fluctuating environments into enzyme kinetics for studying these effects, especially for the chemical steps of the catalytic cycle. It takes into account the complex conformational space of the enzyme−substrate system by first calculating an activation free energy that includes thermally averaged fluctuations of the system and then calculating the recrossing and multidimensional tunneling transmission coefficients as an average over an ensemble of transition state structures and reaction paths. EA-VTST/MT has been successfully applied to several enzyme systems and has been able to provide atomic understanding of the factors that contribute to rate constants (including very large tunneling transmission factors), kinetic isotope effects, and their temperature dependence.

AUTHOR INFORMATION

Corresponding Author

*E-mail: truhlar@umn.edu.

Notes

The authors declare no competing financial interest.

Biographies

Laura Masgrau was born in Manresa (Barcelona) and received a Ph.D. in Chemistry from the Universitat Autònoma de Barcelona in 2002. After a postdoctoral stay at the University of Leicester, U.K. (Profs. M. Sutcliffe and N. Scrutton laboratories), and a second postdoctoral stay at the Institut Pasteur of Paris, she came back to the UAB in 2008 where she works as a senior researcher.

Don Truhlar was born in Chicago and received a Ph.D. in Chemistry from Caltech. Since 1969, he has been on the faculty of the University of Minnesota where he is now Regents Professor of Chemistry, Chemical Physics, Nanoparticle Science and Engineering, and Scientific Computation.

ACKNOWLEDGMENTS

The authors are grateful to our many collaborators (cited in the references) for contributions to this research. L.M. acknowledges financial support from "Programa Banco Santander - UAB" and from the Spanish "Ministerio de Economía y Competitividad" (Project CTQ2011-24292). This work was supported in part by NIH Grant No. 5RC1GM91445-2.

REFERENCES

(1) Karplus, M.; Gao, Y. Q.; Ma, J.; van der Vaart, A.; Yang, W. Protein structural transitions and their functional role. *Philos. Trans. R. Soc. London, Ser. A* **2005**, *363*, 331−355.
(2) Boehr, D. D.; Dyson, H. J.; Wright, P. E. An NMR perspective on enzyme dynamics. *Chem. Rev.* **2006**, *106*, 3055−3079.
(3) Garcia-Viloca, M.; Gao, J.; Karplus, M.; Truhlar, D. G. How enzymes work: Analysis by modern rate theory and computer simulations. *Science* **2004**, *303*, 186−195.
(4) Henzler-Wildman, K. A.; Lei, M.; Thai, V.; Kerns, S. J.; Karplus, M.; Kern, D. A hierarchy of timescales in protein dynamics is linked to enzyme catalysis. *Nature* **2007**, *450*, 913−916.
(5) Hammes, G. G.; Benkovic, S. J.; Hammes-Schiffer, S. Flexibility, diversity, and cooperativity: Pillars of enzyme catalysis. *Biochemistry* **2011**, *50*, 10422−10430.
(6) McGeagh, J. D.; Ranaghan, K. E.; Mulholland, A. J. Protein dynamics and enzyme catalysis: Insights from simulations. *Biochim. Biophys. Acta* **2011**, *1814*, 1077−1092.
(7) Basran, J.; Sutcliffe, M. J.; Scrutton, N. S. Enzymatic H-transfer requires vibration-driven extreme tunneling. *Biochemistry* **1999**, *38*, 3218−3222.
(8) Nagel, Z. D.; Klinman, J. P. A 21st century revisionist's view at a turning point in enzymology. *Nat. Chem. Biol.* **2009**, *5*, 543−550.
(9) Masgrau, L.; Basran, J.; Hothi, P.; Sutcliffe, M. J.; Scrutton, N. S. Hydrogen tunneling in quinoproteins. *Arch. Biochem. Biophys.* **2004**, *428*, 41−51.
(10) Antoniou, D.; Caratzoulas, S.; Kalyanaraman, C.; Mincer, J. S.; Schwartz, S. D. Barrier passage and protein dynamics in enzymatically catalyzed reactions. *Eur. J. Biochem.* **2002**, *269*, 3103−3112.
(11) Limbach, H.-H.; Schowen, K. B.; Schowen, R. L. Heavy atom motions and tunneling in hydrogen transfer reactions: The importance of the pre-tunneling state. *J. Phys. Org. Chem.* **2010**, *23*, 586−605.
(12) Olsson, M. H. M.; Parson, W. W.; Warshel, A. Dynamical contributions to enzyme catalysis: Critical tests of a popular hypothesis. *Chem. Rev.* **2006**, *106*, 1737−1756.
(13) Alhambra, C.; Corchado, J.; Sánchez, M. L.; Garcia-Viloca, M.; Gao, J.; Truhlar, D. G. Canonical variational theory for enzyme kinetics with the protein mean force and multidimensional quantum mechanical tunneling dynamics. Theory and application to liver alcohol dehydrogenase. *J. Phys. Chem. B* **2001**, *105*, 11326−11340.
(14) Pu, J.; Gao, J.; Truhlar, D. G. Multidimensional tunneling, recrossing, and the transmission coefficient for enzymatic reactions. *Chem. Rev.* **2006**, *106*, 3140−3169.
(15) Kuznetsov, A. M.; Ulstrup, J. Proton and hydrogen tunneling in hydrolytic and redox enzyme catalysis. *Can. J. Chem.* **1999**, *77*, 1085−1096.
(16) Antoniou, D.; Basner, J.; Núñez, S.; Schwartz, S. D. Computational and theoretical methods to explore the relation between enzyme dynamics and catalysis. *Chem. Rev.* **2006**, *106*, 3170−3187.
(17) Billeter, S. R.; Webb, S. P.; Iordanov, T.; Agarwal, P. K.; Hammes-Schiffer, S. Hybrid approach for including electronic and nuclear quantum effects in molecular dynamics simulations of hydrogen transfer reactions in enzymes. *J. Chem. Phys.* **2001**, *114*, 6925−6936.
(18) Truhlar, D. G.; Gao, J.; Alhambra, C.; Garcia-Viloca, M.; Corchado, J.; Sánchez, M. L.; Villa, J. The incorporation of quantum effects in enzyme kinetics modeling. *Acc. Chem. Res.* **2002**, *35*, 341−349.

DOI: 10.1021/ar500319e
Acc. Chem. Res. 2015, 48, 431−438

(19) Truhlar, D. G.; Gao, J.; Garcia-Viloca, M.; Alhambra, C.; Corchado, J.; Sánchez, M. L.; Poulsen, T. D. Ensemble-averaged variational transition state theory with optimized multidimensional tunneling for enzyme kinetics and other condensed-phase reactions. *Int. J. Quantum Chem.* **2004**, *100*, 1136−1152.
(20) Truhlar, D. G. Variational transition-state theory and multidimensional tunneling for simple and complex reactions in the gas phase, solids, liquids, and enzymes. In *Isotope Effects in Chemistry and Biology*; Kohen, A., Limbach, H.-H., Eds.; Marcel Dekker: New York, 2006; pp 597−620.
(21) Garcia-Meseguer, R.; Marti, S.; Ruiz-Pernia, J. J.; Moliner, v.; Tuñón, I. Studying the role of protein dynamics in an S_N2 enzyme reaction using free-energy surfaces and solvent coordinates. *Nat. Chem.* **2013**, *5*, 566−571.
(22) Gao, J.; Truhlar, D. G. Quantum mechanical methods for enzyme kinetics. *Annu. Rev. Phys. Chem.* **2002**, *53*, 467−505.
(23) Lin, H.; Truhlar, D. G. QM/MM: What have we learned, where are we, and where do we go from here? *Theor. Chem. Acc.* **2007**, *117*, 185−199.
(24) Senn, H. M.; Thiel, W. QM/MM methods for biomolecular systems. *Angew. Chem., Int. Ed.* **2009**, *48*, 1198−1229.
(25) González-Lafont, A.; Truong, T. N.; Truhlar, D. G. Direct dynamics calculations with neglect of diatomic differential overlap molecular orbital theory with specific reaction parameters. *J. Phys. Chem.* **1991**, *95*, 4618−4627.
(26) Dybala-Defratyka, A.; Paneth, P.; Truhlar, D. G. Quantum catalysis in enzymes. In *Quantum Tunneling in Enzyme-Catalysed Reactions*; Allemann, R., Scrutton, N. S., Eds.; RSC: Cambridge, U.K>, 2009; pp 36−78.
(27) Truhlar, D. G. Tunneling in enzymatic and nonenzymatic hydrogen transfer reactions. *J. Phys. Org. Chem.* **2010**, *23*, 660−676.
(28) Kreevoy, M. M.; Truhlar, D. G. Transition state theory. In *Investigation of rates and mechanisms of reactions*, 4th ed.; Bernasconi, C. F., Ed.; Techniques of Chemistry; Wiley: New York, 1986, Vol. *6*, Pt. 1, pp 13−95.
(29) Truhlar, D. G.; Isaacson, A. D.; Garret, B. C. Generalized transition state theory. In *Theory of Chemical Reaction Dynamics*; Baer, M., Ed.; CRC Press: Boca Raton, FL, 1985; pp 65−136.
(30) Tucker, S. C.; Truhlar, D. G. Dynamical formulation of transition state theory: Variational transition states and semiclassical tunneling. *NATO ASI Ser., Ser. C* **1989**, *267*, 291−346.
(31) Garcia-Viloca, M.; Alhambra, C.; Truhlar, D. G.; Gao, J. Inclusion of quantum-mechanical vibrational energy in reactive potentials of mean force. *J. Chem. Phys.* **2001**, *114*, 9953−9958.
(32) Klippenstein, S. J.; Pande, V.; Truhlar, D. G. Chemical kinetics and mechanisms of complex systems: A perspective on recent theoretical advances. *J. Am. Chem. Soc.* **2014**, *136*, 528−546.
(33) Patey, G. N.; Valleau, J. P. Monte-Carlo method for obtaining the potential of mean force in ionic solution. *J. Chem. Phys.* **1975**, *63*, 2334−2339.
(34) Beutler, T. C.; van Gunsteren, W. F. The computation of a potential of mean force: choice of the biasing potential in the umbrella sampling technique. *J. Chem. Phys.* **1994**, *100*, 1492−1497.
(35) Schenter, G. K.; Garrett, B. C.; Truhlar, D. G. Generalized Transition State Theory in Terms of the Potential of Mean Force. *J. Chem. Phys.* **2003**, *119*, 5828−5833.
(36) Pu, J.; Ma, S.; Gao, J.; Truhlar, D. G. Small temperature dependence of the kinteic isotope effect for the hydride transfer reaction catalyzed by *Escherichia coli* dihydrofolate reductase. *J. Phys. Chem. B* **2005**, *109*, 8551−8556.
(37) Pang, J.; Pu, J.; Gao, J.; Truhlar, D. G.; Allemann, R. K. Hydride transfer reaction catalyzed by hyperthermophilic dihydrofolate reductase is dominated by quantum mechanical tunneling and is promoted by both inter- and intramolecular correlated motions. *J. Am. Chem. Soc.* **2006**, *128*, 8015−8023.
(38) Ferrer, S.; Tuñón, I.; Martí, S.; Moliner, V.; Garcia-Viloca, M.; González-Lafont, A.; Lluch, J. M. A theoretical analysis of rate constants and kinetic isotope effects corresponding to different reactant valleys in lactate dehydrogenase. *J. Am. Chem. Soc.* **2006**, *128*, 16851−16863.
(39) Chatfield, D. C.; Friedman, R. S.; Schwenke, D. W.; Truhlar, D. G. Control of chemical reactivity by quantized transition states. *J. Phys. Chem.* **1992**, *96*, 2414−2421.
(40) Garrett, B. C.; Truhlar, D. G.; Grev, R. S.; Magnuson, A. W. Improved treatment of threshold contributions in variational transition state theory. *J. Phys. Chem.* **1980**, *84*, 1730−1748.
(41) Truhlar, D. G.; Liu, Y.−P.; Schenter, G. K.; Garrett, B. C. Tunneling in the presence of a bath: A generalized transition state theory approach. *J. Phys. Chem.* **1994**, *98*, 8396−8405.
(42) Fernández-Ramos, A.; Ellingson, B. A.; Garrett, B. C.; Truhlar, D. G. Variational transition state theory with multidimensional tunneling. *Rev. Comput. Chem.* **2007**, *23*, 125−232.
(43) Garcia-Viloca, M.; Alhambra, C.; Corchado, J. C.; Sanchez, M. L.;Villa, J.; Gao, J.; Truhlar, D. G. *CHARMMRATE*, version 2.0; University of Minnesota, Minneapolis, 2002. http://comp.chem.umn.edu/charmmrate (accessed Aug. 23, 2014).
(44) Brooks, B. R.; Bruccoleri, R. E.; Olafson, B. D.; States, D. J.; Swaminathan, S.; Karplus, M. CHARMM: A program for macromolecular energy, minmimization, and dynamics calculations. *J. Comput. Chem.* **1983**, *4*, 187−217.
(45) Corchado, J. C.; Chuang, Y.-Y.; Fast, P. L.; Hu, W.-P.; Liu, Y.-P.; Lynch, G. C.; Nguyen, K. A.; Jackels, C. F.; Ramos, A. F.; Ellingson, B. A.; Lynch, B. J.; Melissas, V. S.; Villa, J.; Rossi, I.; Costino, E. L.; Pu, J.; Albu, T. V.; Steckler, R.; Garrett, B. C.; Isaacson, A. D.; Truhlar, D. G. *POLYRATE 9.3.1*; University of Minnesota: Minneapolis, 2005.
(46) Alhambra, C.; Sánchez, M. L.; Corchado, J. C.; Gao, J.; Truhlar, D. G. Erratum to "Quantum mechanical tunneling in methylamine dehydrogenase" [Chem. Phys. Lett. 347 (2001) 512−518]. *Chem. Phys. Lett.* **2002**, *355*, 388−394.
(47) Garcia-Viloca, M.; Alhambra, C.; Truhlar, D. G.; Gao, J. Quantum dynamics of hydride transfer catalyzed by bimetallic electrophilic catalysis: synchronous motion of Mg^{2+} and H^- in xylose isomerase. *J. Am. Chem. Soc.* **2002**, *124*, 7268−7269.
(48) Garcia-Viloca, M.; Truhlar, D. G.; Gao, J. Reaction-path energetics and kinetics of the hydride transfer catalyzed by dihydrofolate reductase. *Biochemistry* **2003**, *42*, 13558−13575.
(49) Garcia-Viloca, M.; Alhambra, C.; Truhlar, D. G.; Gao, J. Hydride transfer catalyzed by xylose isomerase: mechanism and quantum effects. *J. Comput. Chem.* **2003**, *24*, 177−190.
(50) Poulsen, T. D.; Garcia-Viloca, M.; Gao, J.; Truhlar, D. G. Free energy surface, reaction paths, and kinetic isotope effect of short-chain acyl-CoA dehydrogenase. *J. Phys. Chem. B* **2003**, *107*, 9567−9578.
(51) Dybala-Defratyka, A.; Paneth, P.; Banerjee, R.; Truhlar, D. G. Coupling of hydrogenic tunneling to active-site motion in the hydrogen radical transfer catalyzed by a coenzyme B_{12}-dependent mutase. *Proc. Natl. Acad. Sci. U.S.A.* **2007**, *104*, 10774−10779.
(52) Tejero, I.; Garcia-Viloca, M.; González-Lafont, A.; Lluch, J. M.; York, D. M. Enzyme dynamics and tunneling enhanced by compression in the hydrogen abstraction catalyzed by soybean lipoxygenase-1. *J. Phys. Chem. B* **2006**, *110*, 24708−24719.
(53) Ruiz-Pernía, J. J.; Garcia-Viloca, M.; Bhattacharyya, S.; Gao, J.; Truhlar, D. G.; Tuñón, I. Critical role of substrate conformational change in the proton transfer process catalyzed by 4-oxalocronate tautomerase. *J. Am. Chem. Soc.* **2009**, *131*, 2687−2698.
(54) Lans, I.; Peregrina, J. R.; Medina, M.; Garcia-Viloca, M.; González-Lafont, A.; Lluch, J. M. Mechanism of the hydride transfer between *Anabaena* Tyr303Ser FNR_{rd}/FNR_{ox} and $NADP^+/H$. A combined pre-steady-state kinetic/ensemble-averagaed transition-state theory with multidimensional tunneling study. *J. Phys. Chem. B* **2010**, *114*, 3368−3379.
(55) Kanaan, N.; Ferrer, S.; Martí, S.; Garcia-Viloca, M.; Kohen, A.; Moliner, V. Temperature dependence of the kinetic isotope effect in thymidylate synthase. A theoretical study. *J. Am. Chem. Soc.* **2011**, *133*, 6692−6702.
(56) Luk, L. Y. P.; Ruiz-Pernía, J. J.; Dawson, W. M.; Roca, M.; Loveridge, E. J.; Glowacki, D. R.; Harvey, J. N.; Mulholland, A. J.; Tuñón, I.; Moliner, V.; Allemann, R. K. Unraveling the role of protein

DOI: 10.1021/ar500319e
Acc. Chem. Res. 2015, 48, 431−438

dynamics in dihydrofolate reductase catalysis. *Proc. Natl. Acad. Sci. U.S.A.* **2013**, *110*, 16344−16349.
(57) Ruiz-Pernía, J. J.; Luk, L. Y. P.; García-Meseguer, R.; Martí, S.; Loveridge, E. J.; Tuñón, I.; Moliner, V.; Allemann, R. K. Increased dynamic effects in a catalytically compromised variant of *Escherichia coli* dihydrofolate reductase. *J. Am. Chem. Soc.* **2013**, *135*, 18689−18696.
(58) Soriano, A.; Silla, E.; Tuñón, I.; Ruiz-Lopez, M. F. Dynamics and electrostatic effects in enzymatic processes. An analysis of the nucleophilic substitution reaction in haloalkane dehalogenase. *J. Am. Chem. Soc.* **2005**, *127*, 1946−1957.
(59) Hammes-Schiffer, S.; Benkovic, S. J. Relating protein motion to catalysis. *Annu. Rev. Biochem.* **2006**, *75*, 519−541.
(60) Allemann, R. K.; Evans, R. M.; Loveridge, E. J. Probing coupled motions in enzymatic hydrogen tunneling reactions. *Biochem. Soc. Trans.* **2009**, *37*, 349−353.
(61) Klinman, J. P.; Kohen, A. Hydrogen tunneling links protein dynamics to enzyme catalysis. *Annu. Rev. Biochem.* **2013**, *82*, 471−496.
(62) Schnell, J. R.; Dyson, H. J.; Wright, P. E. Structure, dynamics, and catalytic function of dihydrofolate reductase. *Annu. Rev. Biophys. Biomol. Struct.* **2004**, *33*, 119−140.
(63) Falzone, C. J.; Wright, P. E.; Benkovic, S. J. Dynamics of a flexible loop in dihydrofolate reductase from escherichia coli by site-directed mutagenesis. *Biochemistry* **1994**, *33*, 439−442.
(64) Sawaya, M. R.; Kraut, J. Loop and subdomain movements in the mechanism of *Escherichia coli* dihydrofolate reductase: Crystallographic evidence. *Biochemistry* **1997**, *36*, 586−603.
(65) Fierke, C. A.; Johnson, K. A.; Benkovic, S. J. Construction and evaluation of the kinetic scheme associated with dihydrofolate reductase from *Escherichia coli*. *Biochemistry* **1987**, *26*, 4085−4092.
(66) Sikorski, R. S.; Wang, L.; Markham, K. A.; Rajagopalan, P. T. R.; Benkovic, S. J.; Kohen, A. Tunneling and coupled motion in the *Escheichia coli* dihydrofolate reductase catalysis. *J. Am. Chem. Soc.* **2004**, *126*, 4778−4779.
(67) Agarwal, P. K.; Billeter, S. R.; Hammes-Schiffer, S. Nuclear quantum effects and enzyme dynamics in dihydrofolate reductase catalysis. *J. Phys. Chem. B* **2002**, *106*, 3283−3293.
(68) Francis, K.; Kohen, A. Protein motions and the activation of the C-H bond catalyzed by dihydrofolate reductase. *Curr. Opin. Chem. Biol.* **2014**, *21*, 19−24.
(69) Fan, Y.; Cembran, A.; Ma, S.; Gao, J. Connecting protein conformational dynamics with catalytic function as illustrated in dihydrofolate reductase. *Biochemistry* **2013**, *52*, 2036−2049.
(70) Maglia, G.; Allemann, R. K. Evidence for environmentally coupled hydrogen tunneling during dihydrofolate reductase catalysis. *J. Am. Chem. Soc.* **2003**, *125*, 13372−13373.
(71) Luk, L. Y. P.; Loveridge, E. J.; Allemann, R. Different dynamical effects in mesophilic and hyperthermophilic dihydrofolate reductase. *J. Am. Chem. Soc.* **2014**, *136*, 6862−6865.
(72) Brooks, H. B.; Jones, L. H.; Davidson, V. L. Deuterium kinetic isotope effect and stopped-flow kinetic studies of the quinoprotein MADH. *Biochemistry* **1993**, *32*, 2725−2729.
(73) Tresadern, G.; Nuñez, S.; Fauler, P. F.; Wang, H.; Hillier, I. H.; Burton, N. A. Direct dynamics calculations of reaction rate and kinetic isotope effects in enzyme catalyzed reacions. *Faraday Discuss.* **2002**, *122*, 223−242.
(74) Ranaghan, K. E.; Masgrau, L.; Scrutton, N. S.; Sutcliffe, M. J.; Mulholland, A. J. Analysis of classical and quantum paths for deprotonation of methylamine by methylamine dehydrogenase. *ChemPhysChem* **2007**, *8*, 1816−1835.
(75) Masgrau, L.; Roujeinikova, A.; Johannissen, L. O.; Hothi, P.; Basran, J.; Ranaghan, K. E.; Mulholland, A. J.; Sutcliffe, M. J.; Scrutton, N. S.; Leys, D. Atomic description of an enzyme reaction dominated by proton tunneling. *Science* **2006**, *312*, 237−241.
(76) Masgrau, L.; Ranaghan, K. E.; Scrutton, N.; Mulholland, A. J.; Sutcliffe, M. J. Tunneling and classical paths for proton transfer in an enzyme reaction dominated by tunneling: Oxidation of tryptamine by aromatic amine dehydrogenase. *J. Phys. Chem. B* **2007**, *111*, 3032−3047.
(77) Garcia-Viloca, M.; Poulsen, T. D.; Truhlar, D. G.; Gao, J. Sensitivity of molecular dynamics simulations to the choice of the X-ray structure used to model an enzymatic reaction. *Protein Sci.* **2004**, *13*, 2341−2354.
(78) Xue, Q. F.; Yeung, E. S. Differences in the chemical reactivity of individual molecules of an enzyme. *Nature* **1995**, *373*, 681−683.

DOI: 10.1021/ar500319e
Acc. Chem. Res. 2015, 48, 431−438